

# International Journal of Optics and Photonics (IJOP)

A publication of Optics and Photonics Society of Iran (OPSI)



SUMMER-FALL 2016

VOLUME 10

NUMBER 2

<b>Papers' Titles and Authors</b>	<b>Pages</b>
<b>Dynamics of Electrons in Free Electron Laser with Square Core Waveguides</b> Farkhondeh Allahverdi, Amir Hossein Ahmadkhan Kordbacheh, and Farideh Allahverdi	69-79
<b>Optical and Thermal Properties of Mixed Alkali Phosphate Based Glasses</b> Samira Vafaei and Mohammad Hossein Hekmatshoar	81-90
<b>Propagation and Interaction of Electrostatic and Electromagnetic Waves in Two Stream Free Electron Laser in the Presence of Self-Fields</b> Taghi Mohsenpour, Hasan Ehsani Amri, and Zahra Norouzi	91-100
<b>An Analytical Model for Rare Earth Doped Fiber Lasers Consisting of High Reflectivity Mirrors</b> Fateme Kazemizadeh, Rasoul Malekfar, and Fateme Shahshahani	101-110
<b>Photonic Crystal-Based Polarization Converter for Optical Communication Applications</b> Mahmoud Nikoufard and Mohsen Hatami	111-116
<b>Linear and Nonlinear Dust Acoustic Waves in Quantum Dusty Electron-Positron-Ion Plasma</b> Elham Emadi and Hossein Zahed	117-122
<b>Analysis of Protein Concentration Based on Photonic Crystal Ring Resonator</b> Savarimuthu Robinson and Krishnan Vijaya Shanthi	123-130

*In the name of God, the Compassionate, the Merciful*

*International Journal of Optics  
and Photonics  
(IJOP)*

ISSN: 1735-8590

**EDITOR-IN-CHIEF:**

**Habib Tajalli**

University of Tabriz, Tabriz, Iran

**ASSOCIATE EDITOR:**

**Nosrat Granpayeh**

K.N. Toosi University of Technology, Tehran, Iran

**International Journal of Optics and Photonics (IJOP)** is an open access journal published by the Optics and Photonics Society of Iran (OPSI). It is published online semiannually and its language is English. All publication expenses are paid by OPSI, hence the publication of paper in IJOP is **free of charge**.

For information on joining the OPSI and submitting papers, please visit <http://www.ijop.ir>, <http://www.opsi.ir>, or contact the society secretarial office via [info@opsi.ir](mailto:info@opsi.ir).

All correspondence and communication for Journal should be directed to:

**IJOP Editorial Office**

Optics and Photonics Society of Iran (OPSI)

Tehran, 1464675945, Iran

**Phone:** (+98) 21-44292731

**Fax:** (+98) 21-44255936

**Email:** [info@ijop.ir](mailto:info@ijop.ir)

**EDITORIAL BOARD**

**Mohammad Agha-Bolorizadeh**

Kerman University of Technology Graduate Studies,  
Kerman, Iran

**Reza Faraji-Dana**

University of Tehran, Tehran, Iran

**Hamid Latifi**

Shahid Beheshti University, Tehran, Iran

**Luigi Lugiato**

University of Insubria, Como, Italy

**Mohammad Kazem Moravvej-Farshi**

Tarbiat Modares University, Tehran, Iran

**Mahmood Soltanolkotabi**

University of Isfahan, Isfahan, Iran

**Abdonnaser. Zakery**

Shiraz University, Shiraz, Iran

**Muhammad Suhail Zubair**

Texas A & M University, TX, USA

**ADVISORY COMMITTEE**

**Masud Mansuripur**

University of Arizona, AZ, USA

**Jean Michel Nunzi**

University of Angers, Angers, France

**Gang Ding Peng**

University of N.S.W., Sydney, Australia

**Nasser N. Peyghambarian**

University of Arizona, AZ, USA

**Jawad A. Salehi**

Sharif University of Technology, Tehran Iran

**Surendra Pal Singh**

University of Arkansas, AR, USA

# Dynamics of Electrons in Free Electron Laser with Square Core Waveguides

Farkhondeh Allahverdi<sup>a,\*</sup>, Amir Hossein Ahmadkhan Kordbacheh<sup>b</sup>, and Farideh Allahverdi<sup>c</sup>

<sup>a</sup>Department of Physics, Iran University of Science and Technology, Tehran, Iran

<sup>b</sup>Faculty of Physics, Iran University of Science and Technology, Tehran, Iran

<sup>c</sup>Department of Engineering, Andimeshk Branch, Islamic Azad University, Andimeshk, Iran

Corresponding Author Email: [allahverdi.f@gmail.com](mailto:allahverdi.f@gmail.com)

Received: Dec. 6, 2015, Revised: May 8, 2016, Accepted: May 21, 2016, Available Online: Nov. 12, 2016

DOI: 10.18869/acadpub.IJOP.10.2.69

**ABSTRACT-** Due to sensitive and important applications of free-electron laser in industry and medicine, improvement of the power and efficiency of laser has always been emphasized. Therefore, understanding the created field and examining the properties of the field in waveguides with different shapes and studying the sustainability of electrons movement are particularly important. In this study, the behavior of electrons in free-electron laser in the wiggler field by square waveguide with central core is examined which is a new research. Due to the complexity of cross section, the equations governing the field are solved numerically, and magnetostatic fields are calculated and then the changes of Wiggler magnetic field are displayed. Finally, the properties of balanced electron circuits for the first and third harmonics are studied and the strong effect of the third space harmonic on the field is observed in the second magnetic resonance and the obtained results indicate greater volatility of transverse components of velocity.

Since the field intensity on the sides and center of the waveguide and the order of electrons motion are important in determining the laser power and efficiency, studying the behavior of electrons in this research indicates that in the empty space between the two walls, Wiggler magnetic field is minimized and leads to the focus of electron beam. Therefore, the closer is the starting point of the movement of electron to the center of waveguide, the better will be the movement order.

**Keywords:** free electron laser, wiggler field, square waveguide

## I. INTRODUCTION

Free electron laser, is a source of radiation of electromagnetic radiation that can produce a coherent radiation with very high potential in a wide range of electromagnetic spectrum [1]. The most important principle of free electron laser is rotating magnetic field that gives an oscillatory motion to the electron beam, and consequently leads to the acceleration of electrons and development of incident waves. In 1951, Hans Mott from Stanford University calculated the emission spectrum of a beam of electron in a sinuous magnetic field for the first time [2]. This sinuous magnetic field is called Wiggler field. There are many varieties of Wiggler field such as flat, torsion, and coaxial Wiggler field [3-5]. Wiggler field studied in this article like coaxial field is composed of ferrite and dielectric parts that are arranged alternately [6,7]. The presence of a uniform and axial magnetic field also prevents electrostatic repulsion of electrons [8-10].

## II. MAGNETIC STRUCTURE

The waveguide device under study with square cross section has a central cavity (Fig. 1). Like coaxial Wiggler field, the waveguide is composed of ferrite and dielectric parts that are arranged alternately. Uniform magnetic field around the waveguide leads to the development of desirable Wiggler field. The sizes of internal and external walls of the waveguide are assumed to be  $2a$  and  $2b$ . In

order to create appropriate Wiggler field, solenoid is used which provides uniform magnetic field of  $B_0$ .

To obtain the created magneto-static field, Maxwell's equations are used and appropriate boundary conditions are applied.

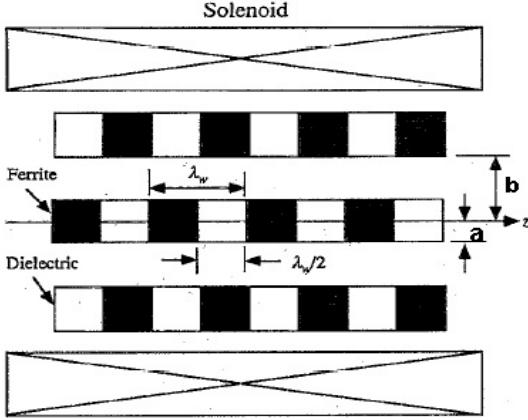


Fig. 1 Cross-section of the waveguide under study

Since there is no current source inside the waveguide, according to [9] and [12], in addition to the divergence, the curl of magnetic field is also zero ( $\nabla \cdot \mathbf{B} = 0$  and  $\nabla \times \mathbf{B} = 0$ ).

The magnetic field can be written as follows, based on magnetic potential  $\varphi$  [11-12]:

$$\mathbf{B} = -\nabla\varphi, \quad \nabla^2\varphi(x, y, z) = 0 \quad (1)$$

System aligned with the z-axis is intermittent with  $\lambda_w$  period; consequently, the magnetic field of  $B_z$  can be expanded as the Fourier series.

$$B_z(x, y, z) = f_0(x, y) + \sum_{n=1}^{\infty} [f_n(x, y) \cos(nk_w z) + g_n(x, y) \sin(nk_w z)] \quad (2)$$

where  $k_w = 2\pi / \lambda_w$ .

$$-\varphi(x, y, z) = f_0(x, y)z + g_0(x, y) + \sum_{n=1}^{\infty} \left[ \frac{1}{nk_w} (f_n(x, y) \sin(nk_w z) - g_n(x, y) \cos(nk_w z)) \right] \quad (3)$$

$$B_x(x, y, z) = -\frac{\partial\varphi(x, y, z)}{\partial x} = \left[ \frac{\partial g_0}{\partial x} + z \frac{\partial f_0}{\partial x} \right] + \sum_{n=1}^{\infty} \left[ \frac{1}{nk_w} \left( \frac{\partial f_n(x, y)}{\partial x} \sin(nk_w z) - \frac{\partial g_n(x, y)}{\partial x} \cos(nk_w z) \right) \right] \quad (4)$$

$$B_y(x, y, z) = -\frac{\partial\varphi(x, y, z)}{\partial y} = \left[ \frac{\partial g_0}{\partial y} + z \frac{\partial f_0}{\partial y} \right] + \sum_{n=1}^{\infty} \left[ \frac{1}{nk_w} \left( \frac{\partial f_n(x, y)}{\partial y} \sin(nk_w z) - \frac{\partial g_n(x, y)}{\partial y} \cos(nk_w z) \right) \right] \quad (5)$$

where  $f$  and  $g$  are related to Fourier transform, and  $\lambda_w$  is the periodicity.

On the other hand, because  $B_x$  and  $B_y$  are alternating with period of  $\lambda_w$ , we can conclude from Eqs. (4)-(5) that  $\frac{\partial f_0}{\partial x} = \frac{\partial f_0}{\partial y} = 0$ . Therefore,

$f_0$  is a numerical constant. By placing (3) in (1), we will have:

$$\left( \frac{\partial^2 g_0}{\partial x^2} + \frac{\partial^2 g_0}{\partial y^2} \right) + \sum_{n=1}^{\infty} \left[ \frac{\sin(nk_w z)}{nk_w} \times \left( \frac{\partial^2 f_n}{\partial x^2} + \frac{\partial^2 f_n}{\partial y^2} - n^2 k_w^2 f_n \right) - \frac{\cos(nk_w z)}{nk_w} \left( \frac{\partial^2 g_n}{\partial x^2} + \frac{\partial^2 g_n}{\partial y^2} - n^2 k_w^2 g_n \right) \right] = 0 \quad (6)$$

The above statement is a Fourier series; therefore, from the uniqueness of expansion coefficients we conclude that:

$$\frac{\partial^2 g_0}{\partial x^2} + \frac{\partial^2 g_0}{\partial y^2} = 0, \quad f_0 = Const \quad (7)$$

$$\frac{\partial^2 f_n}{\partial x^2} + \frac{\partial^2 f_n}{\partial y^2} - n^2 k_w^2 f_n = 0 \quad n \geq 1 \quad (8)$$

$$\frac{\partial^2 g_n}{\partial x^2} + \frac{\partial^2 g_n}{\partial y^2} - n^2 k_w^2 g_n = 0 \quad (9)$$

The sets of Eqs. (7)-(9) are the equations of unknown functions  $f_n(x, y)$  and  $g_n(x, y)$ . By solving these equations, the magnetic field can be obtained through the Eqs. (2), (4), and (5).

### III. DYNAMIC MOVEMENT OF ELECTRONS

In this Section, the orbital motion of electrons in square Wiggler and axial magnetic field are examined. The components of magnetostatic field are as follows (for odd ns):

$$B_x = B_w \sum_{n=1}^{\infty} \frac{\partial f_n(x, y)}{\partial x} \frac{\sin(nk_w z)}{nk_w} = B_w f_x(x, y) \quad (10)$$

$$B_y = B_w \sum_{n=1}^{\infty} \frac{\partial f_n(x, y)}{\partial y} \frac{\sin(nk_w z)}{nk_w} = B_w f_y(x, y) \quad (11)$$

$$B_z = B_0 + B_w \sum_{n=1}^{\infty} f_n(x, y) \cos(nk_w z) = B_0 + B_w f_z(x, y) \quad (12)$$

where  $B_0$  is the constant axial field and  $B_w$  is the Wiggler field.  $f_n(x, y)$  can be calculated by numerical solution of equation (Append X).

The orbital motion of electrons in the static magnetic field of B is investigated by solving Lorentz force equation [4].

$$\frac{d\mathbf{v}}{dt} = \frac{-e}{\gamma mc} \mathbf{v} \times \mathbf{B} \quad (13)$$

where  $\mathbf{v}$  is the velocity,  $-e$  and  $m$  are the electron charge and rest mass, respectively. Given that the  $\mathbf{v} \times \mathbf{B}$  is perpendicular to the velocity  $\mathbf{v}$ , the Lorentz factor  $\gamma$ , is the motion constant factor:  $d\gamma/dt=0$  where

$$\gamma = \left(1 - \frac{v^2}{c^2}\right)^{-1/2} \text{ and } v = |\mathbf{v}| \text{ is the electron}$$

velocity. Moreover, for the electrons path it can be written:  $\frac{d\mathbf{r}}{dt} = \mathbf{v}$ .

The normalized variables  $\bar{\Omega}_0$ ,  $\bar{\Omega}_w$ ,  $\Omega_w$ ,  $\mathbf{v}$ ,  $\bar{R}$ , and T required for calculations are defined as following:

$$\bar{\Omega}_0 = \frac{\Omega_0}{k_w c}, \quad \bar{\Omega}_w = \frac{\Omega_w}{k_w c}, \quad \mathbf{v} = \frac{v}{c},$$

$$\bar{R}_0 = k_w r, \quad \mathbf{T} = k_w ct$$

in which  $\Omega_0 = \frac{eB_0}{\gamma mc}$  and  $\Omega_w = \frac{eB_w}{\gamma mc}$  are cyclotron frequencies. By defining above variables, the components of motion equation will be as the following:

$$\frac{dV_x}{dT} = -\bar{\Omega}_0 V_y - \bar{\Omega}_w V_y f_z + \bar{\Omega}_w V_z f_y \quad (14)$$

$$\frac{dV_y}{dT} = \bar{\Omega}_0 V_x + \bar{\Omega}_w V_x f_z = -\bar{\Omega}_w V_z f_x \quad (15)$$

$$\frac{dV_z}{dT} = \bar{\Omega}_w V_y f_x - \bar{\Omega}_w V_x f_y \quad (16)$$

$$\frac{dR_x}{dT} = V_x \quad (17)$$

$$\frac{dR_y}{dT} = V_y \quad (18)$$

$$\frac{dR_z}{dT} = V_z \quad (19)$$

Equations (14)-(19) are the set of coupled differential equations that are solved numerically using Runge-Kutta algorithm. By solving the equations, the movement path and properties of equilibrium orbits of electrons are obtained.

### IV. ELECTRON ORBITAL THEORY

If the initial condition is chosen so that the transverse motion of electrons in the field  $B_0$  (and at  $B_w \rightarrow 0$ ) is zero, then in the first approximation of Wiggler field and regardless of the statements of the second order  $B_w V_x$  and  $B_w V_y$  in Eqs. (14)-(16), the equations of electron motion will be as follows:

$$\frac{dV_x}{dT} = -\bar{\Omega}_0 V_y + \bar{\Omega}_w V_z f_y$$

$$\frac{dV_y}{dT} = \bar{\Omega}_0 V_x - \bar{\Omega}_w V_z f_x, \quad \frac{dv_z}{dT} = 0 \quad (20)$$

From Eq. (20) we conclude that  $V_z = V_{\parallel}$  and therefore  $R_z = z = V_{\parallel} T$ .

If we assume that Wiggler field is uniform in the transverse direction, in other words if we ignore the changes of  $f_{x,n}$  and  $f_{y,n}$  with respect to  $x$  and  $y$ , by considering the third harmonic we will have:

$$\begin{aligned} \frac{d^2 V_x}{dT^2} + \overline{\Omega}_0^2 V_x &= \overline{\Omega}_w V_{\square} f_{x,1} \sin(V_{\square} T) \overline{\Omega}_0 + \\ &\overline{\Omega}_w V_{\square} f_{x,3} \sin(3V_{\square} T) \overline{\Omega}_0 + \\ &\overline{\Omega}_w V_{\square}^2 f_{y,1} \cos(V_{\square} T) + \\ &3\overline{\Omega}_w V_{\square}^2 f_{y,3} \cos(3V_{\square} T) \end{aligned} \quad (21)$$

Inhomogeneous Eq. (26) can be solved analytically, and the answer to the first condition:

$$V_x(T=0) = V_y(T=0) = 0$$

is as follows:

$$\begin{aligned} V_x(T) &= \frac{\overline{\Omega}_w V_{\square}}{9V_{\square}^4 - 10V_{\square}^2 \overline{\Omega}_0^2 + \overline{\Omega}_0^2} \times \\ &\left[ V_{\square} \left( 9V_{\square}^2 f_{x,1} + 3V_{\square}^2 f_{x,3} - \overline{\Omega}_0^2 f_{x,1} - 3\overline{\Omega}_0^2 f_{x,3} \right) \sin(\overline{\Omega}_0 t) + \right. \\ &f_{x,1} \overline{\Omega}_0 \left( \overline{\Omega}_0^2 - 9V_{\square}^2 \right) \sin(V_{\square} t) + f_{x,3} \overline{\Omega}_0 \\ &\left( \overline{\Omega}_0^2 - V_{\square}^2 \right) \sin(3V_{\square} t) + V_{\square} \\ &\left( 9V_{\square}^2 f_{y,1} + 3V_{\square}^2 f_{y,3} - \overline{\Omega}_0^2 f_{y,1} - 3\overline{\Omega}_0^2 f_{y,3} \right) \\ &\cos(\overline{\Omega}_0 t) + V_{\square} f_{y,1} \left( \overline{\Omega}_0^2 - 9V_{\square}^2 \right) \cos(V_{\square} t) + \\ &\left. 3V_{\square} f_{y,3} \left( \overline{\Omega}_0^2 - V_{\square}^2 \right) \cos(3V_{\square} t) \right] \end{aligned} \quad (22)$$

Moreover, using the above equation and the Eq. (20) we have:

$$\begin{aligned} V_y(T) &= \frac{\overline{\Omega}_w V_{\square}}{9V_{\square}^4 - 10V_{\square}^2 \overline{\Omega}_0^2 + \overline{\Omega}_0^2} \times \\ &\left[ V_{\square} \left( -9V_{\square}^2 f_{x,1} - 3V_{\square}^2 f_{x,3} + \overline{\Omega}_0^2 f_{x,1} + 3\overline{\Omega}_0^2 f_{x,3} \right) \cos(\overline{\Omega}_0 t) + \right. \\ &V_{\square} f_{x,1} \left( 9V_{\square}^2 - \overline{\Omega}_0^2 \right) \cos(V_{\square} t) + \end{aligned}$$

$$\begin{aligned} &3V_{\square} f_{x,3} \left( V_{\square}^2 - \overline{\Omega}_0^2 \right) \cos(3V_{\square} t) + \\ &f_{y,1} \overline{\Omega}_0 \left( \overline{\Omega}_0^2 - 9V_{\square}^2 \right) + \end{aligned} \quad (23)$$

$$\begin{aligned} &\sin(V_{\square} t) + f_{y,3} \overline{\Omega}_0 \left( \overline{\Omega}_0^2 - V_{\square}^2 \right) \sin(3V_{\square} t) + \\ &V_{\square} \left( 9V_{\square}^2 f_{y,1} + 3V_{\square}^2 f_{y,3} - \overline{\Omega}_0^2 f_{y,1} - 3\overline{\Omega}_0^2 f_{y,3} \right) \sin(\overline{\Omega}_0 t) \end{aligned}$$

The above equations are stable solution related to the motion of a single electron. In these equations, the normalized frequencies of  $\overline{\Omega}_0$ ,  $V_{\square}$ , and  $3V_{\square}$  are respectively related to the constant magnetic field  $B_0$ , first harmonic ( $n=1$ ), and third harmonic ( $n=3$ ) of Wiggler field.

## V. RESULTS AND DISCUSSION

Figure 2 shows longitudinal velocity changes of electrons in normalized cyclotron frequency for three groups.

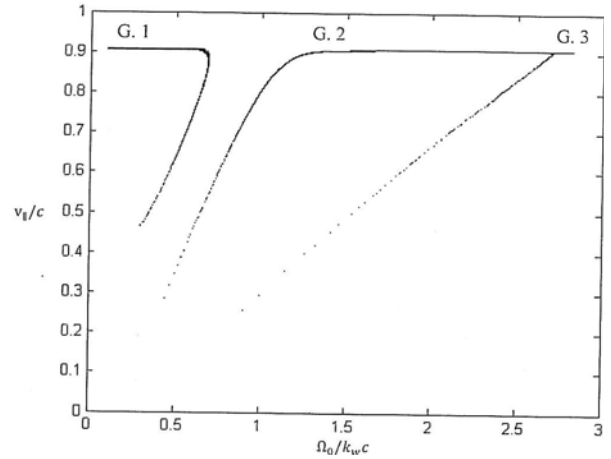


Fig. 2 Variations of normalized axial velocity based on normalized cyclotron frequency.

The orbits of Group I are marked with the condition  $0 < \Omega_0 < k_w V_{\parallel}$ , orbits of group II with the condition  $k_w V_{\square} < \Omega_0 < 3k_w V_{\square}$  and orbits of group III with the condition  $\Omega_0 > 3k_w V_{\square}$ . The third group has appeared due to the presence of the third spatial harmonic for Wiggler field and causes the second resonance in  $\Omega_0 \approx 3k_w V_{\square}$ . The first magneto resonance due to the fundamental component of the wiggler field occurs at  $\overline{\Omega}_0 \approx 0.58$ , whereas the second

magneto resistance originated from the third harmonic is around  $\bar{\Omega}_0 \approx 2.7$ . In  $V_{\square}$  the Space period is equal to wavelength of wiggler and spatial periodicity in  $3V_{\square}$  is a third wavelength of wiggler. The second resonance width is less than the first resonance. It can be concluded that the third harmonic is weaker than first harmonic. Third harmonic more affected on III group and the unaffected on I and II groups. The resonance point transverse velocity reaches its maximum value.

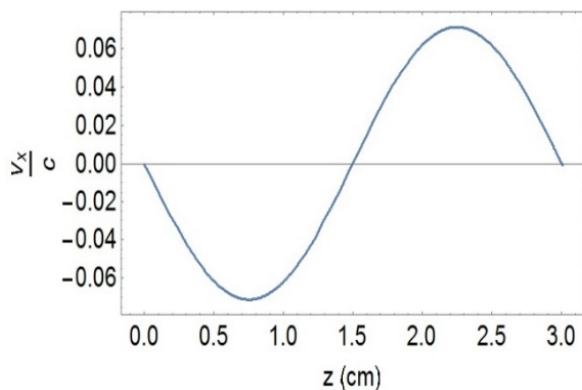


Fig. 3  $V_x$  variations versus  $Z$  for  $\bar{\Omega}_0 = 0.58$

Figures 3 and 4 respectively show the transverse speed of  $V_x$  and  $V_y$  in a period of Wiggler field depending on the distance  $z$ -axis. Periodic changes of speed transverse  $V_x$  and  $V_y$  to  $\bar{\Omega}_0 = 0.58$  (the point where the first magnetic resonance occurs) is equal to one wiggler wavelength (wavelength of main wiggler harmonics). And strong effect on the two groups I and II in the first harmonic resonance magnetic first show.

Figure 5 displays the transverse movement of electrons in two dimensions normalized frequency  $\bar{\Omega}_0 = 0.58$  (first resonator) with initial conditions  $x_0 = 3\text{ cm}$ ,  $y_0 = 0$ , and  $z_0 = 0$ .

As can be seen a period is equal to a third wavelength of Wiggler and electrons that enter the space between the two walls of the waveguide will be movement regular and stable.

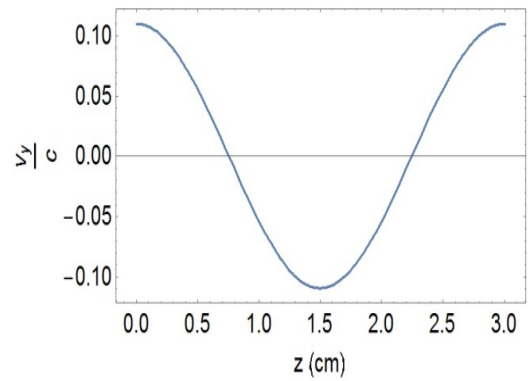


Fig. 4  $V_y$  variations versus  $Z$  for  $\bar{\Omega}_0 = 0.58$

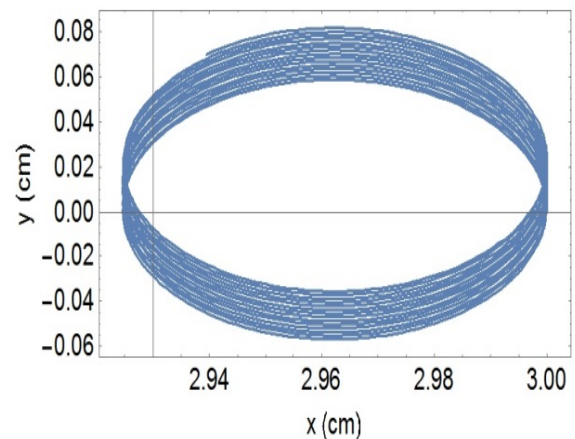


Fig. 5 Transverse direction of electron movement for  $\bar{\Omega}_0 = 0.58$

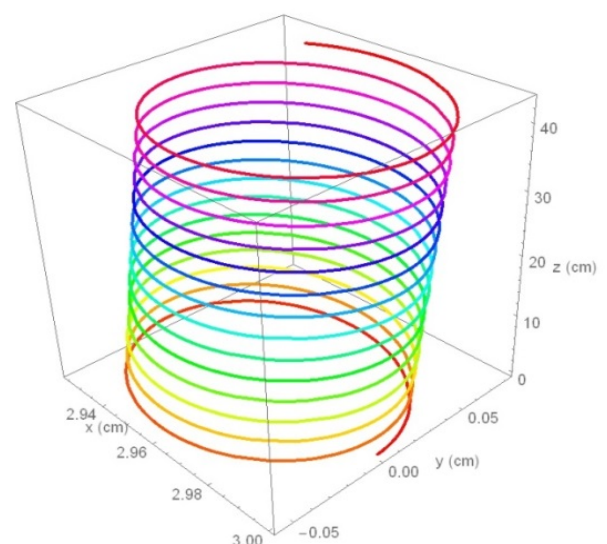


Fig. 6 Three-dimensional direction of electron movement for  $\bar{\Omega}_0 = 0.58$ .

Figure 6 shows the three-dimensional movement of the electrons in terms of the

normalized frequency  $\bar{\Omega}_0 = 0.58$ . It can be seen that the electron orbits in an almost spiral path is limited. As in the prior period equal to the length of the original wiggler harmonic wave and electrons that enter the space between the two walls of the waveguide are moving will be more orderly and stable.

If the initial condition is chosen to move away from the axis of the electron oscillation amplitude is larger and it is possible that the beam is deflected to the side wall.

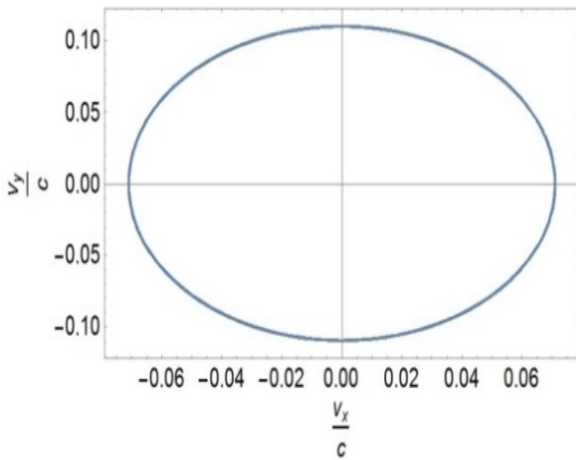


Fig. 7 Transversal speeds of electrons for  $\bar{\Omega}_0 = 0.58$ .

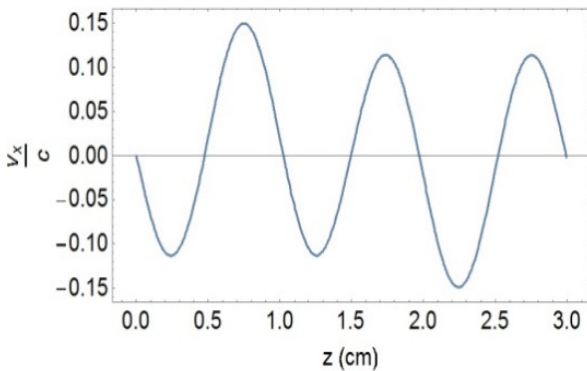


Fig. 8  $V_x$  variations versus  $Z$  for  $\bar{\Omega}_0 = 2.7$

The parameters used to draw these figures are as follows:

$$\bar{\Omega}_0 = 0.58, \quad \bar{\Omega}_w = 0.4, \quad \gamma = 2.37$$

$$a = 2 \text{ cm}, \quad b = 4 \text{ cm}, \quad \lambda_w = 3 \text{ cm}$$

$$x_0 = 3 \text{ cm}, \quad y_0 = 0, \quad z_0 = 0$$

$$v_{x,0} = 0, \quad v_{y,0} = 0.11, \quad v_{z,0} = 0.899$$

where  $2a$  is the size of the inner wall side (core),  $2b$  is the size of the outer wall side,  $\bar{\Omega}_0$  is Cyclotron frequency normalized axial magnetic field.  $\bar{\Omega}_w$  is Normalized cyclotron frequency magnetic field wiggler.  $\lambda_w$  is wavelength of wiggler and  $\gamma$  is Lorentz factor.  $x_0, y_0,$  and  $z_0$  are the initial conditions for the movement of electrons.

Figure 10 shows the transverse motion of the electrons in two dimensions normalized frequency  $\bar{\Omega}_0 = 2.7$  (second resonator) with initial conditions  $x_0 = 3 \text{ cm}, y_0 = 0,$  and  $z_0 = 0$ . As can be seen a period is equal to a third wavelength of Wiggler and electrons that enter the space between the two walls of the waveguide will be movement regular and stable.

Figure 7 displays the transverse velocity curve to the first exacerbation.

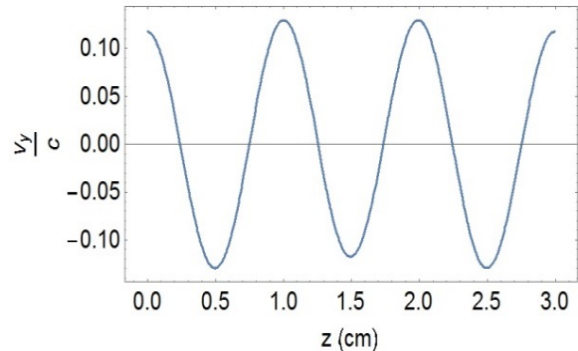


Fig. 9  $V_y$  variations versus  $Z$  for  $\bar{\Omega}_0 = 2.7$ .

Figure 11 shows the three-dimensional motion of the electrons in terms of the normalized frequency  $\bar{\Omega}_0 = 2.7$ . It can be seen that the electron orbits in an almost spiral path is limited. As in the prior period equal to a third wavelength of original wiggler harmonic and electrons that enter the space between the two walls of the waveguide are moving will be more orderly and stable. If the initial condition

is chosen to move away from the axis of the electron oscillation amplitude is larger and it is possible that the beam is deflected to the side wall.

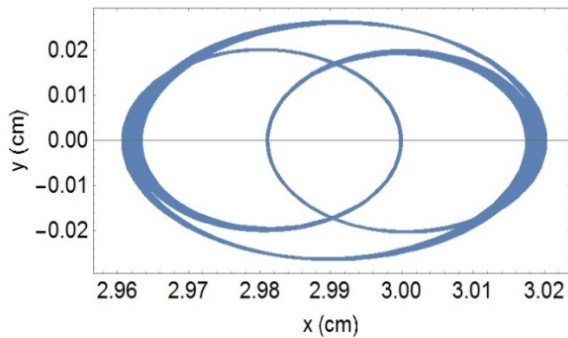


Fig. 10 Transverse direction of electron movement for  $\bar{\Omega}_0 = 2.7$ .

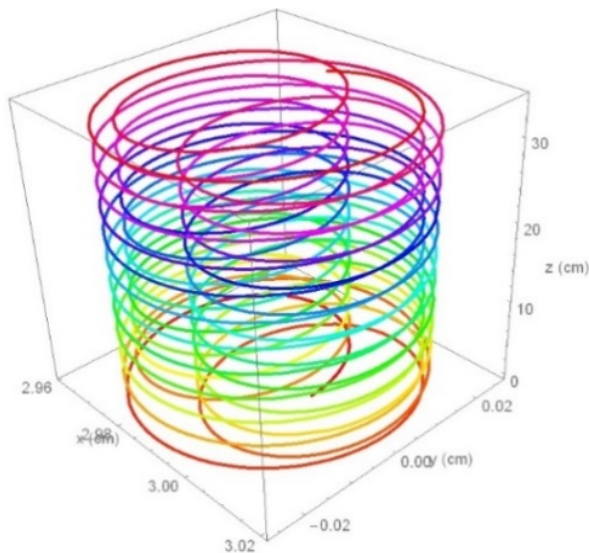


Fig. 11 Three-dimensional direction of electron

Figure 12 displays transverse velocity curve for second resonance  $\bar{\Omega}_0 = 2.7$ . In addition, Figs. (8) and (9), respectively show the transverse velocity of  $v_x, v_y$  in a period of Wiggler field and Figs. (10)-(11) display the movement of electrons in the transverse direction and three dimensions.

It can be concluded from the comparison between Figs. 7 and 12 have large size cannot be changed so it can be considered approximately constant axial velocity.

By comparing all figures, it is obvious that when  $\bar{\Omega}_0 = 0.58$  the spatial period time equals to Wiggler wavelength while when  $\bar{\Omega}_0 = 2.7$  the spatial period time equals to one-third of Wiggler wavelength and indicates the strong effect of the third space harmonic on the field in the second magnetic resonance. It also shows that transverse components of velocity have larger amplitudes.

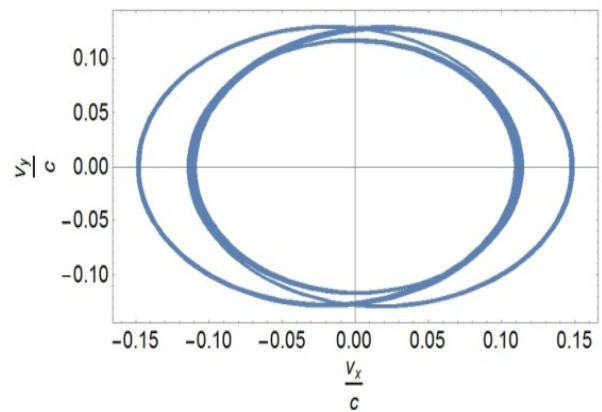


Fig. 12 Transversal speeds of electrons for  $\bar{\Omega}_0 = 2.7$ .

Given the figures of transverse velocity curve it can be found that the transverse velocity cannot change a lot and axial velocity can be considered as nearly constant.

## VI. CONCLUSION

The movement of electrons in free-electron laser in the wiggler field by square waveguide with central core was examined. According to the charts of magnetic fields found that the changes of Wiggler magnetic field at the corners of waveguide are more than those around the waveguide. Moreover, the field components in the empty space between the shell and core have their lowest amount and lead to the concentration of electron beam. Consequently, the closer is the starting point of the movement of electron to the center and the empty space between the two walls, the better will be the movement order.

Examining the results of numerical equations and the related graphs indicate that the spatial

rotation of the transverse speeds with regard to the normalized frequency for the first resonance is one Wiggler wavelength and for the second resonance is one-third of Wiggler wavelength. Moreover, transverse velocity cannot change a lot and axial velocity can be considered to be constant.

## VII. APPENDIX

Boundary conditions related to the problem can be obtained. To do so, different areas will be examined separately.

For example for area  $x \geq 0, y \geq 0$  the problem is solved.

For  $0 \leq x \leq b, y = b$ , from Eq. (2) we have:

$$\begin{aligned} \int_0^{\lambda_w} \int_0^b dx B_z(x, y=b, z) &= \lambda_w \int_0^b dx f_0(x, b) \\ &+ \sum_{n=1}^{\infty} \left[ \int_0^b dx f_n(x, b) \int_0^{\lambda_w} dz \cos(nk_w z) + \right. \\ &\left. \int_0^b dx g_0(x, b) \int_0^{\lambda_w} dz \sin(nk_w z) \right] = \lambda_w b f_0 \end{aligned} \quad (1)$$

For Ferrite parts  $B_z=0$  and for dielectric parts, the average  $B_z$  on  $X$  or  $Y$  equals  $B_{out}$  or  $B_{in}$ .

$$\begin{aligned} \frac{1}{a} \int_0^a dx B_z(x, a, z) &= 0 \\ 0 < z < \frac{\lambda_w}{4}, \quad \frac{3\lambda_w}{4} < z < \lambda_w \end{aligned} \quad (2)$$

$$\frac{1}{a} \int_0^a dy B_z(a, y, z) = B_{in}, \quad \frac{\lambda_w}{4} < z < \frac{3\lambda_w}{4} \quad (3)$$

$$\frac{1}{b} \int_0^b dx B_z(x, b, z) = 0, \quad \frac{\lambda_w}{4} < z < \frac{3\lambda_w}{4} \quad (4)$$

$$\frac{1}{b} \int_0^b dy B_z(b, y, z) = B_{out}$$

$$0 < z < \frac{\lambda_w}{4}, \quad \frac{3\lambda_w}{4} < z < \lambda_w \quad (5)$$

Through the combination of the above equations, we have:

$$B_{out} = 2f_0 \quad (6)$$

$$\frac{1}{b} \int_0^b dx f_n(x, b) = \frac{2B_{out}}{n\pi} \sin\left(\frac{n\pi}{2}\right) \quad (7)$$

$$\int_0^b dx g_n(x, b) = 0 \quad \text{for } 0 \leq x \leq a, y = a \quad (8)$$

$$B_{in} = 2f_0, \frac{1}{a} \int_0^a dx f_n(x, a) = -\frac{2B_{in}}{n\pi} \sin\left(\frac{n\pi}{2}\right) \quad (9)$$

$$\int_0^a dx g_n(x, a) = 0 \quad \text{for } 0 \leq y \leq b, x = b \quad (10)$$

$$\begin{aligned} B_{out} &= 2f_0 \\ \frac{1}{b} \int_0^b dy f_n(b, y) &= \frac{2B_{out}}{n\pi} \sin\left(\frac{n\pi}{2}\right) \end{aligned} \quad (11)$$

$$\int_0^b dy g_n(b, y) = 0 \quad \text{for } 0 \leq y \leq a, x = a \quad (12)$$

$$B_{in} = 2f_0, \frac{1}{a} \int_0^a dx f_n(x, a) = -\frac{2B_{in}}{n\pi} \sin\left(\frac{n\pi}{2}\right) \quad (13)$$

$$\int_0^a dy g_n(a, y) = 0 \quad (14)$$

Similarly, the boundary conditions of other areas can be obtained.

According to the above equations, it is clear that the response  $g_n(x, y)$ , which is true in all circumstances, equals zero then for  $n \geq 0$  we have:  $g_n(x, y) = 0$  and  $n \geq 1, f_{2n}(x, y) = 0$ .

Assuming  $B_{out} = B_{in} = B_0$  then:

$$B_{out} = B_{in} = 2f_0 \tag{15}$$

Thus, the field components are obtained as follows:

$$B_x = \sum_{n=1}^{\infty} \frac{\partial f_n(x,y)}{\partial x} \frac{\sin(nk_w z)}{nk_w} \tag{16}$$

$$B_y = \sum_{n=1}^{\infty} \frac{\partial f_n(x,y)}{\partial y} \frac{\sin(nk_w z)}{nk_w} \tag{17}$$

$$B_z = \frac{B_0}{2} + \sum_{n=1}^{\infty} f_n(x,y) \cos(nk_w z) \tag{18}$$

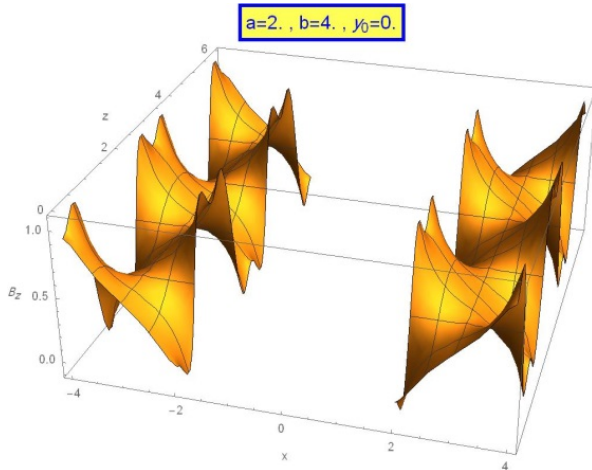


Fig. 1  $B_z$  component of the magnetic field for  $y=y_0=0$ .

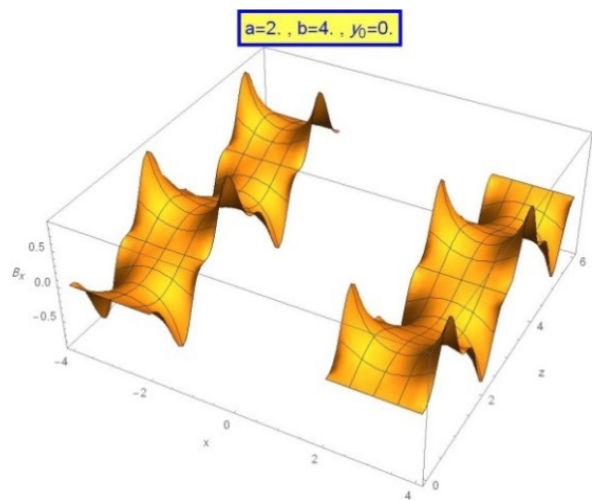


Fig. 2  $B_x$  component of the magnetic field for  $y=y_0=0$ .

From Eq. (8) and the obtained boundary conditions for different areas we will have:

$$\frac{\partial^2 f_n(x,y)}{\partial x^2} + \frac{\partial^2 f_n(x,y)}{\partial y^2} = n^2 k_w^2 f_n(x,y) \tag{19}$$

The average  $f_n(x,y)$  on the outer surfaces is:

$$f_n(x,y) = \frac{2B_0}{n\pi} \sin\left(\frac{n\pi}{2}\right)$$

And the average  $f_n(x,y)$  on the inner surfaces is

$$f_n(x,y) = -\frac{2B_0}{n\pi} \sin\left(\frac{n\pi}{2}\right) \tag{20}$$

For  $x=0, a \leq |y| \leq b: \frac{\partial f_n(x,y)}{\partial x} = 0$  \tag{21}

For  $y=0, a \leq |x| \leq b: \frac{\partial f_n(x,y)}{\partial y} = 0$  \tag{22}

Equation (19) with above boundary conditions is the basic equation governing the system and by solving it and finding  $f_n(x,y)$  the components of the magnetic field can be calculated through relations (16-18).

Now assume that function  $f_n(x,y)$  in the external borders equals  $\frac{2B_0}{n\pi} \sin\left(\frac{n\pi}{2}\right)$  and in

the internal borders equals  $-\frac{2B_0}{n\pi} \sin\left(\frac{n\pi}{2}\right)$ . In

this case, its average will be equal to the given values and therefore it satisfies the boundary conditions. With this assumption, since it is not possible to solve Eq. (19) analytically due to the presence of core in the cross-section of the waveguide (see Fig. 1), the solution to the question can be obtained numerically. In this paper, to solve the Eq. (19) numerically, the *flex PDE* software is used. Then, the obtained numerical solution is called on Mathematica software. Through data interpolation, the magnetic field at any point of the waveguide can be calculated.

Figures 1-3 show different components of the field derived from the numerical method for the constant value of  $y=y_0$  in terms of  $x$  and during the release of  $z$ . As it can be seen, the radial component of the field in the empty

space between the two walls is minimized and leads to the focus of the electron beam. The numerical values of the parameters used in the charts are as  $a=2\text{cm}$ ,  $b=4\text{cm}$ , and  $\lambda_w=3\text{cm}$ . As shown in Fig. (2), since  $B_z$  behavior is minimum at the point  $x=3$ ,  $y=0$  and  $z=0$ , if the electrons enters the waveguide from this region lateral deviations will lower and electrons do not hit the walls. The electrons that enter the waveguide from this area will have more regular and consistent movement.

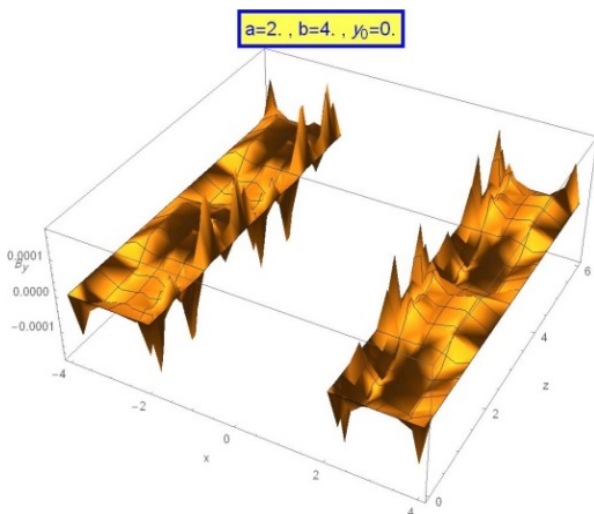


Fig. 3  $B_y$  component of the magnetic field for  $y=y_0=0$

## VIII. REFERENCES

- [1] R.M. Sandhu, "The ubitron, a high-power traveling wave tube based on a periodic beam interaction in unloaded waveguide," IRE Trans. Electron. Devices, Vol. ED-7. PP.231-240, 1960.
- [2] H. Motz, "Applications of the radiation from fast electron beams," J. Appl. Phys. Vol. 22, PP. 527-536, 1951.
- [3] H.P. Freund and J.M. Antonsen, *Principle of Free Electron Laser* Chapman and Hall, 2<sup>nd</sup> Ed. 1992.
- [4] H. Bluem, R.H. Jackson, H.P. Freund, D.E. Pershing, and V.L. Granatstein, "Demonstration of a new free-electron laser harmonic interaction," Phys. Rev. Lett. Vol. 67, PP. 824-827, 1991.
- [5] R.H. Jackson, H.P. Freund, D.E. Pershing, and J.M. Taccetti, *Nuclear Instruments and Methods in physics research*, section A Vol. 429 PP.116-120, 1999.
- [6] P. Sprangle, "Fast-wave interaction with a relativistic electron beam," J. Plasma phys. Vol. 11, PP.299-308, 1974.
- [7] P. Sprangle and V.L. Granatstein, "Stimulated cyclotron resonance scattering and production of powerful submillimeter radiation," Appl. Phys. Lett. Vol. 25, PP. 377-387, 1974.
- [8] H.P. Freund and A.K. Ganguly, "Electron orbits in a Free-Electron lasers with helical wiggler and axial guide magnetic fields," IEEE J. Quantum Electron. Vol. QE-21. PP. 1073-1083, 1985.
- [9] H.P. Freund, R.H. Jackson, D.E. Pershing, and J.M. Taccetti, "Nonlinear theory of the free electron laser based upon a coaxial hybrid wiggler," Phys. Plasmas, Vol.1, pp. 1046-1059, 1994.
- [10] H. Dreicer, "Kinetic theory of an electron-photon gas," Phys. Fluids, Vol. 7, pp. 735-741, 1964.
- [11] E. Jerby, "Traveling-wave free-electron laser," Phys. Rev. A, Vol. 44, pp.703-715, 1991.
- [12] A. Kordbacheh, R. Ghahremaninezhad, and B. Maraghechi, "The analysis of single-electron orbits in a free electron laser based upon a rectangular hybrid wiggler," Phys Plasma, Vol. 19, pp. 141-148, 2012.



**Farkhondeh Allahverdi** received the MSc degree in Solid State Physics from Science and Technology University, Tehran, Iran in 2015 . Her research fields are Free Electron Laser and Quantum.



**Amir Hossein Ahmadkhan Kordbacheh** received the PhD degree in Solid State Physics from Amir Kabir University, Tehran, Iran. His research field is free electron laser, To survey electronic structure, magnetic and optical properties of materials using density functional theory and methods of optical sensor. Dr. Kordbacheh is assistant professor in Science and Technology, University of Tehran, Iran



**Farideh Allahverdi** received the MSc degree in electrical engineering from Islamic Azad University Science and Research Branch in 2008 and she is PhD Student in Electrical Engineering in Islamic Azad University, Ahvaz, Iran.

**THIS PAGE IS INTENTIONALLY LEFT BLANK.**

## SCOPE

Original contributions relating to advances, or state-of-the-art capabilities in the theory, design, applications, fabrication, performance, and characterization of: Lasers and optical devices; Laser Spectroscopy; Lightwave communication systems and subsystems; Nanophotonics; Nonlinear Optics; Optical Based Measurements; Optical Fiber and waveguide technologies; Optical Imaging; Optical Materials; Optical Signal Processing; Photonic crystals; and Quantum optics, and any other related topics are welcomed.

## INFORMATION FOR AUTHORS

International Journal of Optics and Photonics (IJOP) is an **open access** Journal, published online semiannually with the purpose of publication of original and significant contributions relating to photonic-lightwave components and applications, laser physics and systems, and laser-electro-optic technology. Please submit your manuscripts through the Web Site of the Journal (<http://www.ijop.ir>). Authors should include full mailing address, telephone and fax numbers, as well as e-mail address. Submission of a manuscript amounts to assurance that it has not been copyrighted, published, accepted for publication elsewhere, and that it will not be submitted elsewhere while under consideration.

## MANUSCRIPTS

The electronic file of the manuscript including all illustrations must be submitted. The manuscript must be in double column with the format of **IJOP Paper Template** which for ease of application all over the world is in MS-Word 2003. The manuscript must include an abstract. The abstract should cover four points: statement

of problem, assumptions, and methods of solutions, results and conclusion or discussion of the importance of the results. All pages, including figures, should be numbered in a single series. The styles for references, abbreviations, etc. should follow the IJOP format. For information on preparing a manuscript, please refer to the IJOP webpage at: <http://www.ijop.ir>.

Prospective authors are urged to read this instruction and follow its recommendations on the organization of their paper. References require a complete title, a complete author list, and first and last pages cited for each entry. All references should be archived material such as journal articles, books, and conference proceedings. Due to the changes of contents and accessibility over time, Web pages must be referenced as low as possible.

**Figure captions** should be sufficiently clear so that the figures can be understood without referring to the accompanying text. Lettering and details of the **figures** and **tables** should be large enough to be readily legible when the drawing is reduced to one-column width of the double column article. **Axes of graphs** should have self-explanatory labels, not just symbols (e.g., Electric Field rather than E). **Photographs** and **figures** must be glossy prints in electronic files with GIF or JPEG Formats.

**Article Keywords** are mandatory and must be included with all manuscripts. Please choose approximately 4 to 8 keywords which describe the major points or topics covered in your article.

## COPYRIGHT TRANSFER FORM

Authors are required to sign an IJOP copyright transfer form before publication. *Authors must submit the signed copyright form with their manuscript.* The form is available online at <http://www.ijop.ir>

